

Green Chemistry

Accepted Manuscript



This is an *Accepted Manuscript*, which has been through the Royal Society of Chemistry peer review process and has been accepted for publication.

Accepted Manuscripts are published online shortly after acceptance, before technical editing, formatting and proof reading. Using this free service, authors can make their results available to the community, in citable form, before we publish the edited article. We will replace this *Accepted Manuscript* with the edited and formatted *Advance Article* as soon as it is available.

You can find more information about *Accepted Manuscripts* in the [Information for Authors](#).

Please note that technical editing may introduce minor changes to the text and/or graphics, which may alter content. The journal's standard [Terms & Conditions](#) and the [Ethical guidelines](#) still apply. In no event shall the Royal Society of Chemistry be held responsible for any errors or omissions in this *Accepted Manuscript* or any consequences arising from the use of any information it contains.

ARTICLE

Good's buffers as a basis for developing self-buffering and biocompatible ionic liquids for biological research

Cite this: DOI: 10.1039/x0xx00000x

Received 00th January 2012,
Accepted 00th January 2012

DOI: 10.1039/x0xx00000x

www.rsc.org/

Mohamed Taha, Francisca A. e Silva, Maria V. Quental, Sónia P. M. Ventura, Mara G. Freire, and João A. P. Coutinho*

This work reports a promising approach on the development of novel self-buffering and biocompatible ionic liquids for biological research in which the anions are derived from biological buffers (Good's buffers, GB). Five Good's buffers (Tricine, TES, CHES, HEPES, and MES) were neutralized with four suitable hydroxide bases (1-ethyl-3-methylimidazolium, tetramethylammonium, tetraethylammonium, and tetrabutylammonium) producing 20 Good's buffer ionic liquids (GB-ILs). The presence of the buffering action of the synthesized GB-ILs was ascertained by measuring their pH-profiles in water. Moreover, a series of mixed GB-ILs with wide buffering ranges were formulated as universal buffers. The impact of GB-ILs on bovine serum albumin (BSA), here used as a model protein, is discussed and compared with more conventional ILs using spectroscopic techniques, such as infrared and dynamic light scattering. They appear to display, in general, a greater stabilizing effect on the protein secondary structure than conventional ILs. A molecular docking study was also carried out to investigate the binding sites of GB-IL ions to BSA. We further used the QSAR-human serum albumin binding model, logK(HSA), to calculate the binding affinity of some conventional ILs/GB-ILs to HSA. The toxicity of the GB and GB-ILs was additionally evaluated revealing that they are non-toxic. Finally, the GB-ILs were also shown to be able to form aqueous biphasic systems when combined with aqueous solutions of inorganic or organic salts, and we tested their extraction capability for BSA. These systems were able to extract BSA with outstanding extraction efficiencies of 100 % in a single step for the GB-IL-rich phase, and, as a result, the use of GB-ILs-based ABS for the separation and extraction of other added-value biomolecules is highly encouraging and worthy of further investigation.

Introduction

Room temperature ionic liquids (RTILs) have been considered as a new type of non-aqueous solvents for chemical synthesis, biocatalysis, electro-chemical devices, polymerization, engineering fluids, and other purposes. This wide variety of applications is a major result of their unusual and tunable physicochemical properties.¹⁻⁵ ILs are salts that remain in the liquid state below the boiling point of water (100 °C). They are characterized by a high ionic conductivity, high chemical/thermal stability, non-flammability, and high solubility for a large range of materials. Several studies have shown that some ILs, either pure or in aqueous solution, can increase the stability of biomolecules like proteins, enzymes and DNA, which is expressed in the vast number of manuscripts published in this field.⁵⁻⁹ The cations and anions of biocompatible ILs are usually more complex than common salts, such as NaCl. The IL cations are often nitrogen-based,

namely alkylammonium, dialkylimidazolium, alkylpyridinium and alkylpyrrolidinium, or phosphorous-containing compounds, such as the widely employed tetralkylphosphoniums. IL anions can be halides, nitrates, sulfates, alkylsulfates, alkylsulfonates, [BF₄]⁻, [PF₆]⁻, [CH₃CO₂]⁻, [CF₃CO₂]⁻, [Tf₂N]⁻, [R₂PO₄]⁻, among others.

Proteins remain in their native (folded) state under physiological conditions, whereas their denatured (unfolded) state is induced by thermal or chemical unfolding. The effects of ions on protein folding, enzyme activity, and protein crystallization, are typically described by the Hofmeister series.¹⁰ Although it has been accepted that salt ions exert their effects indirectly by changing the water structure, recent results have questioned this model and shown that in most cases a direct interaction of the salt ions with the protein is involved.¹¹ A particularly useful aspect of ILs results from their combination between chaotropic cations and kosmotropic anions, that were

shown previously to stabilize proteins.¹² Another important aspect of ILs is that their polarity and hydrophobicity can be tuned by varying the alkyl side-chain length of the cations and by a proper selection of the cation core or anion nature. There are several reports showing that the enzyme activity increases with the IL hydrophobicity up to a maximum, and then decreases with a further increase on the IL hydrophobicity.¹² In contrast, there are also some conflicting studies reporting a relatively high enzyme stability and activity in hydrophilic ILs.¹²

Proteins' stability is strongly affected by the proton activity of the supporting solution and has an optimum pH that can be adjusted by the addition of a proper biological buffer. It is generally accepted that, at appropriate concentrations, hydrophilic ILs tend to, fully or partly, dissociate in aqueous solutions and into ions which form neutral or very weakly basic solutions. Certainly, this pattern is not always true because there are some functionalized ILs that work as Lewis acidic or basic catalysts. Adding a buffer into aqueous IL solutions, when dealing with protein stability, will not provide an adequate pH control since the ILs acidity or basicity could swamp the buffer effect. Therefore, it is crucial to look for alternative pH control methods, and in particular in the design of ILs with buffering characteristics. Until recently, few works reported the synthesis of ILs with buffering action.¹³⁻¹⁶ Nevertheless, those buffer-like ILs are not recommended for biochemical research because their anions are not inert. A number of criteria are required for a buffer to be used in biological and biochemical studies.¹⁷ They must be chemically inert, should not interfere with metal ion-protein binding, be non-toxic, do not absorb light in the UV-visible region, be commercially available at a low cost, their pK_a values should be between 6.0 and 8.0 and should do not vary with temperature, and present high water solubility and low solubility in organic solvents. Good and his research team have designed biological buffers (Good's buffers, GB) that fit these criteria.¹⁷

Good's buffers are zwitterionic amino acid derivatives, and they are the most widely used biological buffers. It was suggested that these Good's buffers act as kosmotropic substances (strongly hydrated molecules)¹⁸⁻²² and protein structure stabilizers.¹⁸⁻²⁰ Since Good's buffers are zwitterionic compounds, they can be used as anion or cation radicals of ILs. In this study, our major goal is to evaluate the possibility of using Good's buffers as anions in the development of novel ionic liquids and that would control the pH and can stabilize proteins. This would create new protein stabilizing ionic liquids with self-buffering characteristics. The Good's buffers adopted in this work are Tricine, TES, CHES, HEPES, and MES. We have selected 1-ethyl-3-methylimidazolium ([Emim]⁺), tetramethylammonium ([N₁₁₁₁]⁺), tetraethylammonium ([N₂₂₂₂]⁺), and tetrabutylammonium ([N₄₄₄₄]⁺) as cations because of their favourable characteristics.^{13, 23} The impact of the GB-ILs on protein structure and stability is discussed and compared with more conventional ILs. The ability of these ILs

to form aqueous biphasic systems, when combined with aqueous solutions of inorganic or organic salts, to be used in novel separation and extraction processes is also investigated and was ascertained here by their extraction efficiencies for a model protein. The toxicity of the GB and GB-ILs was also assessed using the Microtox[®] toxicity test.^{24, 25}

Experimental

Materials

The buffers, CHES (purity > 99 wt%), HEPES (purity > 99.5 wt%), MES (purity > 99 wt%), Tricine (purity > 99 wt%), and TES (purity > 99 wt%), were purchased from Sigma-Aldrich Chemical Co. The hydroxide-based compounds, [Emim][OH] (10 wt% in H₂O), [N₁₁₁₁][OH] (25 wt% in H₂O), [N₂₂₂₂][OH] (25 wt% in H₂O), and [N₄₄₄₄][OH] (40 wt% in H₂O), were also supplied by Sigma-Aldrich Chemical Co. (USA). Sodium hydroxide pellets from Eka Chemicals were obtained from Sigma-Aldrich Chemical Co. (USA). The salts, sodium sulfate (Na₂SO₄, purity ≈99.99 wt%) and potassium citrate tribasic monohydrate (C₆H₅K₃O₇·H₂O, purity ≥ 99 wt%) were obtained from Sigma-Aldrich Chemical Co. (USA). BSA/fraction V, pH = 7.0, was obtained from Acros Organics. Methanol (HPLC grade, purity > 99.9%) was obtained from Fisher Scientific (UK). Acetonitrile (purity > 99.7%) was supplied from Lab-Scan (Ireland). Purified water passed through a reverse osmosis and a Milli-Q plus 185 water purifying system was used in all experiments.

Synthesis and characterization of Good's buffer ionic liquids

Aqueous solutions of 1-ethyl-3-methylimidazolium, tetramethylammonium, tetraethylammonium, or tetrabutyl ammonium hydroxides were added drop-wised to a slightly excess of an equimolar buffer aqueous solution. The reaction mixture was stirred at ambient conditions for about 12 h. The mixture was then evaporated at 50-60 °C under reduced pressure and which gives rise to a viscous liquid. A mixture of acetonitrile and methanol 1:1 was added to the viscous liquid and stirred vigorously at room temperature for 1 h. The solution was then filtered to remove any excess buffer. The solvent mixture was evaporated and the GB-IL product was dried in vacuum (10 Pa) for 3 days at room temperature. The water content in each GB-IL was measured by Karl-Fischer (KF) titration, using a KF coulometer (Metrohm Ltd., model 831), and it was found to be less than 0.05 wt% in all samples. The chemical structures of the GB-ILs were confirmed by ¹H and ¹³C NMR spectroscopy (Bruker AMX 300) operating at 300.13 and 75.47 MHz, respectively. Chemical shifts are expressed in δ (ppm) using tetramethylsilane (TMS) as internal reference. The melting points were measured by differential scanning calorimetry (DSC), using a Perkin Elmer DSC-7 instrument (Norwalk, CT), and with a heating rate = 5 °C·min⁻¹ and N₂ flow = 40 mL·min⁻¹. The characterization data (NMR chemical shifts and melting temperatures) are given in the Table S1, in the ESI[†].

Potentiometric titrations

The pH titration profiles were determined in a double-walled glass vessel using an automatic titrator (Metrohm 672) equipped with a dosimat 655 and a pH glass electrode (Metrohm 6.0229.100) for pH measurements in aqueous solutions. The pH electrode was calibrated in aqueous solution with two standard buffers of pH 4.0 and 7.0. The temperature of the titration vessel was controlled at 20 °C by a thermostatic water bath. For measuring the pH profile of GB-ILs in water, 10 mL of each GB-ILs at 0.05 M were freshly prepared in water and titrated with 0.05 M NaOH/HCl under continuous magnetic stirring. At least two repeated measurements were performed for the determination of each pH profile.

Dynamic light scattering (DLS) measurements

To estimate the hydrodynamic radius (RH) with increasing temperature from (25 to 75) °C, DLS measurement were carried out using a ZetasizerNano ZS (Malvern Instruments Ltd., UK). The average RH was calculated using the instrument software from the scattering intensity data. The light source is a He-Ne laser light (4mW) with a fixed wavelength, $\lambda = 633$ nm, and the measurements were conducted at a fixed scattering angle of 173°. The instrument is provided with a thermostatic sampling chamber able to control the temperature in the range from 0 °C to 90 °C. The samples for DLS analysis consist of 20 mg·cm⁻³ of BSA diluted in aqueous solutions of (0.05 and 0.5) M conventional ILs/GB-ILs at pH= 7.4. They were then incubated at 25 °C for 4 h to attain the equilibrium, and a bubble free sample of around 1.3 cm³ in a square glass cuvette with round aperture (PCS8501) was used for the DLS measurements.

Infrared measurements

Attenuated total reflectance (ATR) Fourier transform infrared (FTIR) spectra of 60 mg of BSA in (0.05 and 0.5) M conventional ILs/GB-ILs aqueous solutions were obtained on an ABB MB3000 FTIR spectrometer using a PIKE MIRacle™ with a single reflection diamond/ZnSe crystal plate. The measured spectral region was between 400 and 4000 cm⁻¹ with a resolution of 4 cm⁻¹ and with 150 scans. At least 5 1 measurements were carried out for each sample. The second-derivative spectra of the amide I (1653 cm⁻¹) region were used as peak position guides for the Gaussian curve-fitting analysis. The relative amount of each secondary structure component was determined by computing the areas of the bands assigned to a particular substructure (i.e., α -helices, β -sheets, and turns). Both second-derivative and curve fitting were performed using the PeakFit v4.0 software (AISN software Inc.).

Phase diagrams of aqueous biphasic systems

The binodal curve of each ABS was determined through the cloud point titration method at 25 (\pm 1) °C and atmospheric pressure. The experimental procedure was validated in previous reports.^{26, 27} Repetitive drop-wise addition of the aqueous salt solution to the IL solution was carried out until the detection of a cloudy biphasic solution, followed by the drop-wise addition

of water until detection of a monophasic region. This procedure was carried under constant stirring. Each mixture composition was determined by the weight quantification of all components added within an uncertainty of $\pm 10^{-4}$ g (using an analytical balance, Mettler Toledo Excellence XS205 DualRange).

The tie-lines (TLs) of each phase diagram, and at the mixtures compositions for which the extraction of BSA was carried out, were determined by a gravimetric method originally described by Merchuk et al.²⁸ The selected mixture, at the biphasic regime, was prepared by weighting the appropriate amounts of IL + salt + water, vigorously stirred, and further submitted to centrifugation for 10 min and at controlled temperature (25 °C). After centrifugation, the sample was left in equilibrium for more 10 min at (25 \pm 1) °C to guarantee the equilibration of the coexisting phases at the target temperature. After this period, each phase was carefully separated and weighted. Each individual TL was determined by the application of the lever-arm rule to the relationship between the weight of the top and bottom phases and the overall system composition, and as previously described.^{26, 27} For this approach each experimental binodal curve was previously fitted as described elsewhere.^{26, 27} All the calculations considering the mass fractions or molality of the citrate-based salt were carried out discounting the complexed water.

Extraction of BSA

The ternary mixtures used in the partitioning experiments of BSA were gravimetrically prepared at a fixed and common mixture composition: (22.4 \pm 1.3) wt % of IL + (25.6 \pm 2.6) wt% of salt. The aqueous solution added contained BSA at a concentration of *circa* 0.5 g·dm⁻³. Each mixture was vigorously stirred, centrifuged for 10 min, and left to equilibrate for at least 10 min at 25 (\pm 1) °C to achieve the complete BSA partitioning between the two phases. After, a careful separation of the two phases was performed and the amount of BSA in each phase was quantified by SE-HPLC (Size Exclusion High-Performance Liquid Chromatography). Each phase was diluted at a 1:10 (v:v) ratio in a phosphate buffer saline solution before injection. A Chromaster HPLC (VWR, Hitachi) coupled with an UV-Vis detector. RP-HPLC was performed on an analytical column (25 cm \times 2 mm i.d., 25 μ m), Lichrospher 100 RP-18 from Merck. A 100 mM phosphate buffer in MiliQ water (mobile phase) was run isocratically with a flow rate of 1 mL·min⁻¹. The column oven temperature was kept constant at 25 °C as well as the autosampler temperature. The injection volume was of 25 μ L. The wavelength was set at 280 nm whereas the retention time of BSA was found to be 9.31 min within an analysis time of 24 min. The quantification of the BSA was carried out by external standard calibration method in the range of 0.001 to 1 g·dm⁻³ of protein. At least three independent biphasic mixtures for each GB-IL-based system were prepared and 3 samples of each phase were quantified. The interference of the salts and ILs with the quantification method was also ascertained and blank control samples were always initially analyzed.

The percentage extraction efficiency of BSA, $EE_{BSA}\%$, is the percentage ratio between the amount of protein in the IL-rich aqueous phase to that in the total mixture, and is defined according to Eq. 1,

$$EE_{BSA}\% = \frac{[BSA]_{IL} \times w_{IL}}{[BSA]_{IL} \times w_{IL} + [BSA]_{Salt} \times w_{Salt}} \quad (1)$$

where $[BSA]$ is the concentration of protein, w is the weight of each phase, and the subscripts IL and Salt represent the IL- and salt-rich phases, respectively.

Microtox® toxicity tests

The Microtox® test was adopted to evaluate the toxicity of the GBs and the corresponding GB-ILs towards the marine bacterium *Vibrio fischeri* by measuring its luminescence inhibition. The bacterium was exposed to a series of diluted solutions of each compound, ranging from 0 to 81.9 %, being 100% the concentration of the stock solutions previously prepared. After 30 min of exposure to each compound, the light output of the bacterium was assessed and compared to the light output of the blank control, enabling the calculation of the EC_{50} values at 30 min through the Microtox® Omni™ Software version 41.²⁹

Computational details

The molecular docking between BSA and GB-IL ions was studied with the Auto-dock Tools vina 1.5.4 program,³⁰ which is much more efficient than Autodock 4. This program is widely used in docking studies. The crystalline structure of BSA (PDB, 3v03)³¹ was used in the docking. The center of the grid was placed at the center of mass of BSA ($90.398 \times 28.894 \times 23.482$) Å, and the grid dimension was ($84 \times 56 \times 82$) Å, which is large enough to cover the whole protein. The partial atomic charges of the cations $[Emim]^+$, $[N_{1111}]^+$, $[N_{2222}]^+$, and $[N_{4444}]^+$, as well as of the Tricine zwitterion and its anion were calculated in water with a polarizable continuum model (IEF-PCM) using density functional theory (DFT) with the B3LYP method with the standard 6-311++G(d,p) basis set and using the natural bond orbital (NBO) as implemented in the Gaussian 09 package.³² The calculated partial atomic charges were used in the docking. The best binding model for ligand docking was decided based on the one with the lowest objective function.

For the QSAR-serum albumin binding model, $\log K(HSA)$, the molecular geometries of GB-ILs were optimized using the AM1 semiempirical method using HyperChem (Version 8.0.7, Hypercube, Inc, USA, <http://www.hyper.com>) program. The AM1 optimization was preceded by the Polak-Rebieri algorithm to reach a 0.01 root mean square gradient. The COSMO files of GB-ILs were obtained by single point density functional calculations. DFT/COSMO calculations were performed using the BP functional, the SVP basis set, and the RI-DFT method, as implemented in the TURBOMOLE 6.1 program package.³³ The COSMO files were then used to obtain $\log K(HSA)$ using the COSMOtherm software.³³

Results and discussion

Tricine is a *N*-substituted glycine derivative whereas the other buffers are *N*-substituted taurine derivatives. The 20 natural amino acids and taurine were previously used as anions for the synthesis of functionalized-ILs known as amino acid ionic liquids (AA-ILs).^{34, 35} The approach here attempted consisted on the synthesis of buffer-like ILs, GB-ILs. The synthesis procedure follows the one used in preparing AA-ILs, through a simple neutralization reaction between GBs and $[Emim][OH]/[N_{1111}][OH]/[N_{2222}][OH]/[N_{4444}][OH]$. The synthesis pathway for GB-ILs is shown in Figure 1. It is noteworthy to mention that all imidazolium salts ($[Emim][Tricine]$, $[Emim][TES]$, $[Emim][HEPES]$, $[Emim][MES]$, and $[Emim][CHES]$), $[N_{4444}][CHES]$, and $[N_{2222}][TES]$ are highly viscous liquids at room temperature. The GB-ILs $[N_{1111}][TES]$, $[N_{1111}][CHES]$, $[N_{2222}][CHES]$, $[N_{2222}][HEPES]$, $[N_{4444}][TES]$, $[N_{4444}][MES]$ are solid at room temperature yet with melting points below 100 °C. Moreover, $[N_{4444}][Tricine]$ and $[N_{4444}][HEPES]$ have melting temperatures around 100 °C. On the other hand, $[N_{2222}][MES]$, $[N_{1111}][Tricine]$, $[N_{1111}][MES]$, $[N_{1111}][HEPES]$, and $[N_{2222}][Tricine]$ have melting points higher than 100 °C, and thus these five salts alone are not contemplated in the general ILs category. However, since there are the IL aqueous solutions that are useful as media for biological studies rather than molten ILs these last compounds are of equal interest. The detailed melting temperatures of all the synthesized GB-ILs are reported in ESI†.

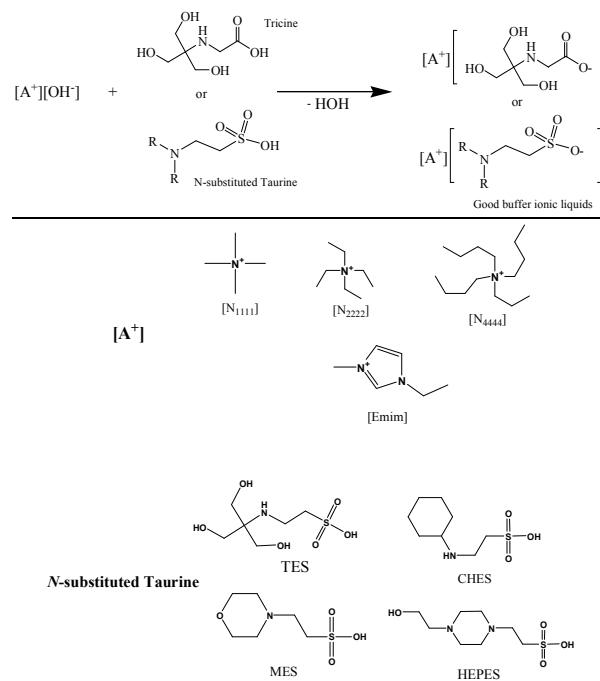


Fig. 1 The synthesis pathway for Good's buffer ionic liquids.

GB-ILs buffer potential

To evaluate the potential of these new ionic liquids as buffers in aqueous media their pH profiles have been measured. Fig. 2(a) shows the pH profiles of the investigated Good's buffers, namely of $[N_{1111}][GB]$. The remaining profiles for other buffers are shown in Figure S1 in the ESI†. The GBs display two pK_a 's: the first dissociation constant (pK_{a1}) is due to the deprotonation of the carboxylic or sulfonic group, and the second dissociation is due to deprotonation of the protonated amino group (pK_{a2}). The inflection point at high pH of those titration curves is due to the deprotonation/protonation of the amine group of the GB/GB-ILs. The region of moderate slope before the inflection point is the buffer region. In this region, the pH is regulated by the equilibrium between the deprotonated and protonated forms. At the middle of this region, the concentrations of these two species are equal, and thus, according to the Henderson-Hasselbalch equation, the pH will be equal to the pK_{a2} and the buffering capacity is maximum at this point.

It can be clearly seen in Fig. 2(a) (as well as in Figure S1 in ESI) that all the GB-ILs dissolved in water present buffering regions which are identical to those of the corresponding Good's buffers. Table S2 in the ESI† reports the mid-point pH buffering. The mid-point pH values and the buffering pH ranges of GB and GB-ILs in water are almost the same. Interestingly, the buffer capacities of GB-ILs, except for Tricine-ILs, are generally higher than the corresponding GBs.

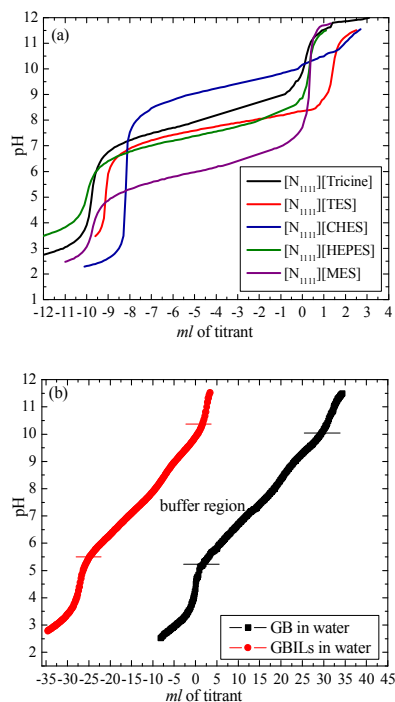


Fig. 2 (a) The pH profiles of the investigated $[N_{1111}][GB]$ in pure water at $(20 \pm 1)^\circ\text{C}$. (b) The pH profiles of the universal buffers; GB refers to a mixture of MES, HEPES, and CHES, whereas GB-ILs refers to $[N_{1111}][MES]$, $[N_{1111}][HEPES]$, and $[N_{1111}][CHES]$.

It is not unusual for enzyme activity assays to span a wide pH range. In order to maintain the solution buffer capacity, different buffers can be used to cover the entire pH range. This raises serious questions about how to distinguish the buffers influences from the pH effects since many buffers have been found to be less inert than originally believed. Using a single buffering solution with a broad working pH range would greatly simplify the interpretation of enzyme activity data. There are few universal-buffers with a wide working pH range (2-12) that have been reported.³⁶ They are, however, formulated with buffers that interact with proteins, or chelate metal-ions.³⁶ Three of the five investigated GBs have negligible metal-binding affinity making them suitable for formulating biocompatible universal buffers, *i.e.*, MES, HEPES, and CHES. An universal Good's buffer (UGB) composed of MES, HEPES, and CHES buffers was firstly tested in aqueous solution. The pH profile of UGB was nearly linear from pH 5.2 to 10.0 (Fig. 2b). A second formulated universal buffer composed of $[N_{1111}][MES]$, $[N_{1111}][HEPES]$, and $[N_{1111}][CHES]$ was tested in water with a linear profile from pH 5.2 to 10.4. It is important to notice that the pH range of GB-ILs can be controlled by the adequate choice of the anion (Good's buffer).

Protein stability in GB-ILs

To explore the effect of GB-ILs on the protein stability, the most important blood protein, bovine serum albumin (BSA), was chosen as a model protein due to its enormous well-known functional applications.³⁷ BSA is widely employed as a carrier for antibody generation in immunoassays for hormones, other metabolites, or drugs, and thus, it serves as a model protein for protein-drug interaction studies.³⁷ BSA is also widely used to determine the quantity of other proteins.³⁷ Furthermore, BSA is used as a functional constituent in pharmaceutical and health care products,³⁷ in cells separation and as a nutrient in cell culture,³⁷ and in the protection of other enzymes during the digestion of DNA.³⁷

The native conformation of a protein is the thermodynamically most-stable and active state. However, an increase in temperature can disturb this stable conformation. When the proteins are submitted to heating, the molecular vibrations of the peptide backbone accelerate and, consequently, the intermolecular hydrogen bonds and hydrophobic interactions are interrupted leading to the protein denaturation. The thermal denaturation temperature (T_d) of a protein is the temperature at which the protein denatures. Upon unfolding, the BSA protein undergoes reversible and irreversible conformational changes. The reversible structure changes occur in the temperature range from (25 to 50) $^\circ\text{C}$, while the irreversible change happens above its denaturation temperature ($\sim 55^\circ\text{C}$).¹⁸⁻²⁰ By heating the protein above its T_d , the hydrophobic residues became exposed to the solvent and interact with other hydrophobic residues on different protein chains leading to the formation of aggregates, which changes the protein size and that can be effectively monitored by dynamic light scattering (DLS).¹⁸⁻²⁰ We present a comparison

between the thermal stability and structure of BSA in some conventional ionic liquids ([Emim]Br, [N₁₁₁₁]Br, [N₂₂₂₂]Br, and [N₄₄₄₄]Br), and GB-ILs ([Emim][Tricine], [N₁₁₁₁][Tricine], [N₂₂₂₂][Tricine] and [N₄₄₄₄][Tricine]) at pH = 7.4. The denaturation curves of BSA (protein size vs. temperature) are plotted in Fig. S2 in the ESI†. The T_d values were obtained by plotting the protein size (hydrodynamic radius, R_h) as a function of temperature. The temperature at which both the size and the intensity start to increase significantly was taken as the beginning of the denaturation process and reported as T_d .¹⁸⁻²⁰ The T_d value of BSA in 0.05 M Tricine at pH = 7.4 is 56 °C while the T_d values of BSA in 0.05 M of [Emim]Br, [N₁₁₁₁]Br, [N₂₂₂₂]Br, and [N₄₄₄₄]Br are 56 °C, 56 °C, 48 °C, and 56 °C, respectively. Increasing the concentrations of [N₁₁₁₁]Br, [N₂₂₂₂]Br, and [Emim]Br to 0.5 M leads to an enhancement of the thermal stability of BSA to 60 °C, 57 °C, and 58 °C, respectively. The DLS results show that [N₄₄₄₄]Br leads to the aggregation of BSA, T_d = 48 °C, and increasing the [N₄₄₄₄]Br concentration to 0.5 M further decreases the T_d to 40 °C. The impact of the corresponding GB-ILs on the thermal stability of BSA is similar to that of traditional ILs. However, one of the advantages of using GB-ILs over the traditional ILs is that no buffer is needed to be added to control the pH of the protein solution. At room temperature and at 0.05 M of conventional/GB-ILs, we have noticed that increasing the alkyl side chains of the ammonium cation leads to an increase in the protein size. This change in R_h is significant at high IL concentrations, namely 0.5 M; e.g., the size ratio of BSA in [N₄₄₄₄][Tricine]/[N₁₁₁₁][Tricine] equals approximately to 2.7, indicating that BSA forms oligomeric species.

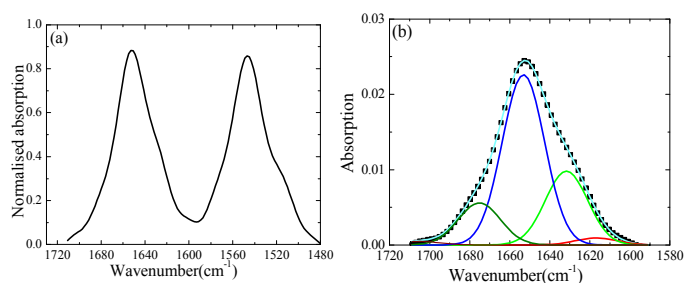


Fig. 3 (a) IR spectra of the amide I and II regions of 60 mg·cm⁻³ of BSA in water and in 0.05 M Tricine at pH 7.4. (b) Gaussian curve-fitting analysis of amide I spectra in 0.05 M Tricine at pH 7.4.

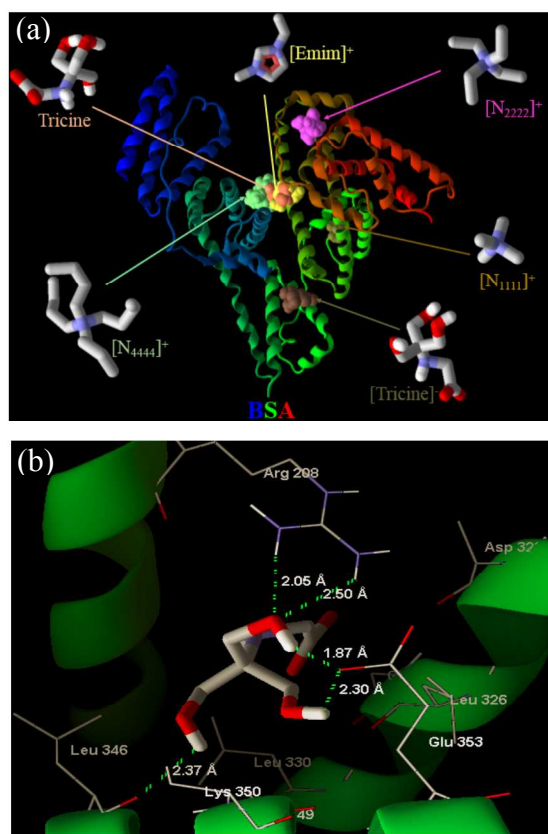
To get further insights on the BSA-(GB-IL) interactions, IR spectra of the amide I & II of BSA in the above-mentioned conventional ILs and GB-ILs at pH = 7.4 have been measured. The amide I band arises from the C=O stretching vibrations and the amide II band is a combination of N—H bending with C—H stretching vibrations. These peaks are the most important vibrational bands of the protein backbone. The amide I and II bands of BSA in 0.05 M Tricine at pH = 7.4 appear at (1653 and 1547) cm⁻¹, respectively (Fig. 3a). Curve fitting was carried out for the amide I to obtain information about the BSA secondary structure in the presence of conventional ILs and

GB-ILs (Table 1). The amide I of BSA in 0.05 M Tricine at pH = 7.4 (Fig. 3b) shows five bands at (1616, 1631, 1653, 1675, and 1697) cm⁻¹. In water, the bands in 1615 cm⁻¹, 1631 cm⁻¹, 1653 cm⁻¹, 1675 cm⁻¹, and 1697 cm⁻¹ are assigned to intermolecular β -sheet, intramolecular β -sheet, α -helix, turn, and antiparallel β -sheet, respectively.³⁸⁻⁴⁰ The obtained α -helix, intermolecular β -sheet, intramolecular β -sheet, turn, and antiparallel β -sheet of free BSA are respectively 57.6 %, 2.4 %, 25.0 %, 14.2 %, and 0.8 %. The secondary structure of BSA is mainly composed of α -helices (57.6 %). The α -helix value is in good agreement with those previously reported in the open literature (56.8 %).⁴¹ The helicity of BSA in the studied conventional ILs is lower than that of IL free except in 0.05 M [N₄₄₄₄][Tricine] (58.2 %), and increasing the IL concentration decreases the α -helices amount. The α -helix content of BSA in the conventional ILs follows the order: [N₄₄₄₄]Br > [N₂₂₂₂]Br > [N₁₁₁₁]Br > [Emim]Br. Interestingly, the helicity of BSA in GB-ILs (Table 1) is greater than that in the conventional ILs, and increasing the GB-ILs concentration increases the α -helices content. The α -helices of BSA in GB-ILs follow the order: [N₄₄₄₄][Tricine] > [Emim][Tricine] > [N₂₂₂₂][Tricine] > [N₁₁₁₁][Tricine]. Thus, the BSA aggregation in presence of [N₄₄₄₄][Tricine] that was observed by the DLS measurements suggests that BSA undergoes aggregation through hydrophobic surface or near-surface without unfolding. This affinity to aggregate rather than global unfolding is in good agreement with other studies.⁴²⁻⁴⁵

A molecular docking study was performed in order to further investigate the binding sites of the GB-ILs ions in BSA. The BSA contains 583 amino acid residues in a single polypeptide chain with three homologous domains (I, II, and III). It has 17 disulfide bridges and one free SH group, which divides the protein into 9 loops (L1-L9) in a roughly heart-shaped structure.⁴⁶ The hydrophobic residues are located in the interior of BSA, while the polar residues appear at the protein surface. The binding sites and binding free energies of Tricine zwitterion, Tricine anion, [N₁₁₁₁]⁺, [N₂₂₂₂]⁺, [N₄₄₄₄]⁺, and [Emim]⁺ with BSA were determined (Fig. 4a). The lowest binding energy mode was searched out from 9 different conformers for each ligand. The Autodock scoring function includes hydrogen bonding, electrostatic interactions and short-range van der Waals, loss of entropy upon ligand binding, and solvation energies terms. Tricine zwitterion was found adjacent to the residues, Arg196, Arg458, Asp108, Ser192, and His145 (domain IB); while the residues found next to Tricine anion are Glu353, Arg208, Asp323, Gly327, Leu346, Leu330, Ala349, and Lys350 (domain IIB). We can clearly see that the binding sites of Tricine anion are different from the Tricine zwitterion. Tricine zwitterion was found to have 5 hydrogen bonds with the adjacent amino acids (Arg458, Asp108, Ser192, and His145); and Tricine anion also

Table 1. Secondary structure analysis (infrared spectra) for BSA in conventional ILs/GB-ILs at pH 7.4

Amide I components	Tricine 0.05 M	[N ₁₁₁₁]Br		[N ₂₂₂₂]Br		[N ₄₄₄₄]Br		[Emim]Br		[N ₁₁₁₁][Tricine]		[N ₂₂₂₂][Tricine]		[N ₄₄₄₄][Tricine]		[Emim][Tricine]	
		0.05 M	0.5 M	0.05 M	0.5 M	0.05 M	0.5 M	0.05 M	0.5 M	0.05 M	0.5 M	0.05 M	0.5 M	0.05 M	0.5 M	0.05 M	0.5 M
Inter β-sheet	2.4	2.9	4.4	3.4	2.9	3.7	1.6	1.9	8.4	3.2	—	—	—	—	—	—	—
Intra β-sheet	25.0	25.6	25.7	23.9	26.1	22.6	25.6	27.0	24.6	25.6	28.5	26.4	29.5	25.5	27.5	25.2	27.5
α-helix	57.6	57.0	49.3	57.0	53.3	58.2	57.5	55.5	48.3	58.5	59.8	60.9	61.5	62.0	65.7	61.6	63.4
turn	14.2	14.5	18.3	15.7	14.2	15.5	14.5	15.6	15.3	12.7	11.7	12.7	9.0	12.5	6.8	13.2	9.1
antiparallel β-sheet	0.8	—	2.3	—	3.5	—	0.8	—	3.4	—	—	—	—	—	—	—	—

**Fig. 4.** (a) Molecular docking of BSA with GB-ILs ions. (b) The hydrogen bond formation between the Tricine anion and BSA.

forms 5 hydrogen bonds with Leu346, Glu353, and Arg208 residues, respectively (Fig. 4b). The residues Arg256, Ile289, Ala290, Leu27, Val240, and Tyr149 (domain IIA) exist near to the [N₁₁₁₁]⁺; and those found nearby [N₂₂₂₂]⁺ are Glu125, Phe133, Lys136, Leu122, and Leu115 (domain IB). The residues found next to the [N₄₄₄₄]⁺ are Ile455, Thr190, Tyr451, Leu454, Lys431, and Ser428 (domain IIIA); and those nearby [Emim]⁺ are His145, Arg458, Arg196, and Ala193 (domain IB). The binding free energy of BSA-Tricine zwitterion interaction is -4.6 kcal·mol⁻¹, while for BSA-Tricine anion is -4.5 kcal·mol⁻¹. On the other hand, the binding free energies of [N₁₁₁₁]⁺, [N₂₂₂₂]⁺, [N₄₄₄₄]⁺, and [Emim]⁺ with BSA are, respectively, (-2.5, -4.0, -4.9, and -4.1) kcal·mol⁻¹. Thus, the binding energy increases with an increase on the alkyl-chain length. The binding affinity of the cations to BSA follows the

order: [N₄₄₄₄]⁺ > [Emim]⁺ > [N₂₂₂₂]⁺ > [N₁₁₁₁]⁺. It seems that more hydrophobic cations have a higher serum bovine binding capability. It is important to notice that the ion pair formation between the GB anions and cations probably occurs in water. By treating the ion pair as neutral molecules, the QSAR-human serum albumin binding model, logK(HSA), was used to calculate the binding affinity of the investigated conventional ILs/GB-ILs to human serum albumin (Table 2). BSA is usually used as a template of human serum albumin because their amino acid sequence is very similar (75% identity and 87% similarity).⁴⁷ It is clear that the GB-ILs have relatively high serum protein binding as compared to the corresponding bromide ILs, and the binding affinity follows the cations order: [N₄₄₄₄]⁺ > [N₂₂₂₂]⁺ > [Emim]⁺ > [N₁₁₁₁]⁺. Interestingly, the trend in of the α-helices of BSA in the tetraalkylammonium cations is similar to that in the GB-ILs. This observation indicates that GB-ILs stabilize the protein not by their effects on the water structure but by their direct binding with the protein. In fact, this protein has specific binding sites that can bind with bioactive substances, such as fatty acids, and which increase its thermal stability.⁴⁸ The polarity and hydrophobicity of these new ILs can be modified by varying the alkyl side-chain length of the cations since these properties have a large impact on the protein stability.

Table 2. The predicted logK(HSA) of GB-ILs

GB-ILs	QSPR- logK(HSA)	GB-ILs	QSPR- logK(HSA)
[N ₁₁₁₁]Br	-1.6323	[N ₁₁₁₁][Tricine]	-1.1752
[N ₂₂₂₂]Br	-1.1049	[N ₂₂₂₂][Tricine]	-0.6939
[N ₄₄₄₄]Br	0.1408	[N ₄₄₄₄][Tricine]	0.5338
[Emim]Br	-1.3955	[Emim][Tricine]	-0.8960

GB-ILs ABS formation

Taking into account the advantages of GB-ILs when dealing with proteins, these compounds could also be used for extraction and separation processes involving proteins, enzymes and antibodies. It is well known that adding organic/inorganic salts into aqueous solution of imidazolium-, pyridinium, pyrrolidinium- and piperidinium-based ILs, ABS can be formed.^{49, 50} There is today a growing research field addressing the applications of IL-based ABS for the extraction of a wide range of valuable compounds, such as alkaloids, drugs, amino

acids, proteins, metals, etc.^{3, 50-54} The potential of GB-ILs to form ABS, aiming at their use in extraction and separation processes or biphasic reactions, was here evaluated. The results collected in this work show that adding inorganic/organic salts to aqueous solution of tetrabutylammonium-based GB-ILs lead to the formation of promising ABS.

The experimental data corresponding to the ternary phase diagrams determined in this work are presented in Table S3 and S4 in ESI†. In all the studied ABS, either with Na₂SO₄ or K₃C₆H₅O₇, the top phase corresponds to the IL-rich aqueous phase while the bottom phase is mainly composed of salt and water. Fig. 5 presents the phase diagrams obtained for several [N₄₄₄₄][GB] and two salts. In addition, the phase diagram for the ABS composed of [N₄₄₄₄][Cl] + K₃C₆H₅O₇ was taken from literature and it is included for comparison purposes.⁵⁵

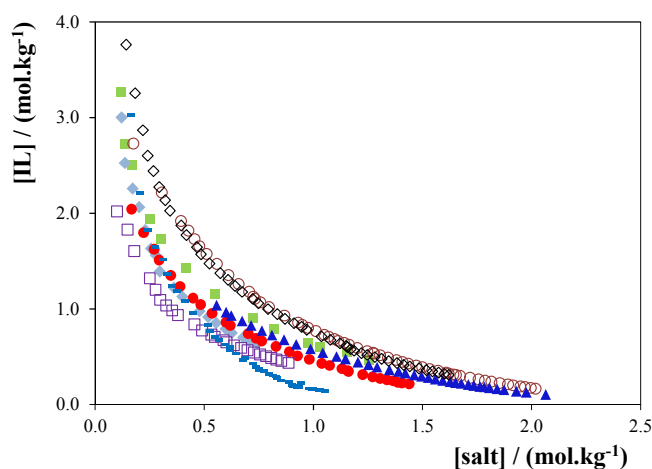


Fig. 5 Ternary phase diagrams for the systems composed of IL + K₃C₆H₅O₇ + water at 25 °C and atmospheric pressure: (○) [N₄₄₄₄][Tricine], (◆) [N₄₄₄₄][MES], (■) [N₄₄₄₄][TES], (●) [N₄₄₄₄][HEPES], (◄) [N₄₄₄₄][CHES], and (◇) [N₄₄₄₄][Cl].⁵⁵ Ternary phase diagrams for the systems composed of IL + Na₂SO₄ + water at 25 °C and atmospheric pressure: (□) [N₄₄₄₄][MES], and (▲) [N₄₄₄₄][Tricine].

In order to understand the influence of the buffer structure on the phase diagrams behaviour, the binodal curves are expressed in terms of molality units to avoid the differences

Table 3 Percentage extraction efficiencies of serum bovine albumin, $EE_{BSA}\%$, in the ABS composed of [N₄₄₄₄][GB] + K₃C₆H₅O₇ at 25 °C, and respective data for the tie-lines (TLs) and tie-line lengths (TLLs). Initial mixture compositions are represented as [IL]_M and [Salt]_M whereas [IL]_{IL} and [IL]_{Salt} are the composition of IL and salt at the IL-rich phase, respectively, and *vice-versa*.

IL	Weight fraction composition / (wt %)						TLL ^a	$EE_{BSA}\%$
	[IL] _M	[Salt] _M	[IL] _{IL}	[Salt] _{IL}	[IL] _{Salt}	[Salt] _{Salt}		
[N ₄₄₄₄][Tricine]	22.45	25.96	39.19	14.48	9.45	35.43	35.57	100
[N ₄₄₄₄][HEPES]	22.55	23.72	54.17	3.68	6.60	33.82	56.31	100
[N ₄₄₄₄][TES]	20.89	28.14	51.73	5.79	11.01	35.30	50.29	100

$$^a \text{TLL} = \sqrt{([\text{Salt}]_{IL} - [\text{Salt}]_{\text{Salt}})^2 + ([IL]_{IL} - [IL]_{\text{Salt}})^2}$$

that would arise from different molecular weights. The two phase regions are localized above the binodal curves. The binodal curves clearly show that the less hydrophilic buffers, as CHES or MES, are more easily salted-out when compared to the more hydrophilic ones (HEPES, TES, or Tricine). Furthermore, the inorganic salt (Na₂SO₄) with a high charge density anion is a stronger salting-out agent than the organic salt (C₆H₅K₃O₇·H₂O) – visible in the formation of ABS composed of [N₄₄₄₄][Tricine] and [N₄₄₄₄][MES]. Fig. 5 also compares the phase behaviour of [N₄₄₄₄][GB] with the more conventional IL-based ABS constituted by [N₄₄₄₄][Cl] and C₆H₅K₃O₇. The results show that [N₄₄₄₄][GB] are more easily salted-out than [N₄₄₄₄][Cl]. Given the characteristics of the GB-ILs, they seem to be ideally suited for preparation of ABS for separation and extraction of high-value biomolecules.

Extraction of BSA using GB-IL-based ABS

In order to use the previous highlighted advantages of GB-ILs, as self-buffering compounds, protein stabilizers, and their abilities to form ABS, we have evaluated them in the extraction of BSA in ABS composed of [N₄₄₄₄][Tricine]/[N₄₄₄₄][TES] / [N₄₄₄₄][HEPES] + K₃C₆H₅O₇, at *ca.* pH 7. These systems have been chosen because they offer a high buffer capacity at pH 7. The organic salt (C₆H₅K₃O₇) was chosen to perform the extraction of BSA due to its biodegradable and non-toxic nature. Table 3 presents the extraction efficiencies of BSA. The initial mixture compositions, the compositions of each phase (tie-lines) and respective tie-line lengths are also shown in Table 3. The tie-lines are also depicted in Fig. S3 in ESI†, while the correlation parameters used to describe the experimental binodal data are given in Table S5, also in the ESI†. In all the studied examples it was observed that the IL-rich phase is able to completely extract the protein with extraction efficiencies of 100%. In fact, no protein was detected at the salt-rich phase. Moreover, from a weight balance it is possible to establish that there are no “losses” of protein, either by precipitation or denaturation.

Table 4 EC₅₀ (mg·dm⁻³) with the respective 95% confidence limits (within brackets) of GBs and the corresponding GB-ILs after 30 minutes of exposure of the marine bacterium *Vibrio Fischeri*

Compound	EC ₅₀ (mg·dm ⁻³) at 30 min (lower limit; upper limit)	Compound	EC ₅₀ (mg·dm ⁻³) at 30 min (lower limit; upper limit)
MES	214.74 (95.65; 333.83)	Tricine	6040.57 (3515.55; 8566.59)
[N ₁₁₁₁][MES]	-	[N ₁₁₁₁][Tricine]	1036.05 (695.37; 1376.73)
[N ₂₂₂₂][MES]	44302.87 (43842.40; 44763.34)	[N ₂₂₂₂][Tricine]	1232.51 (379.69; 2085.33)
[N ₄₄₄₄][MES]	550.49 (438.82; 662.16)	[N ₄₄₄₄][Tricine]	180.24 (172.20; 188.28)
[Emim][MES]	14766.73 (4468.36; 25065.11)	[Emim][Tricine]	562.27 (180.63; 943.90)
TES	661.17 (236.32; 1086.02)	HEPES	8684.08 (4697.83; 12670.32)
[N ₁₁₁₁][TES]	-	[N ₁₁₁₁][HEPES]	15149.61 (8490.34; 21808.88)
[N ₂₂₂₂][TES]	21072.78 (16689.50; 25456.05)	[N ₂₂₂₂][HEPES]	5589.69 (1368.15; 9811.24)
[N ₄₄₄₄][TES]	271.55 (263.46; 279.63)	[N ₄₄₄₄][HEPES]	216.60 (141.95; 291.26)
[Emim][TES]	3377.36 (2082.43; 4672.29)	[Emim][HEPES]	5731.82 (4483.90; 6979.74)
CHES	16497.82 (10222.58; 22773.07)		
[N ₁₁₁₁][CHES]	222.25 (215.78; 228.72)		
[N ₂₂₂₂][CHES]	238.08 (229.20; 246.96)		
[N ₄₄₄₄][CHES]	179.77 (152.05; 207.49)		
[Emim][CHES]	362.29 (347.70; 376.87)		

GB-ILs toxicities

The EC₅₀ values determined after 30 min of exposure and the respective 95% confidence limits are reported in Table 4. The EC₅₀ data at 30 min were adopted to guarantee that a long enough exposition time is used.⁵⁶ The results show that, in general, the GB-ILs here prepared possess a non-toxic character to the bacterium as indicated by their high EC₅₀ data, ranging from 44302.87 mg·dm⁻³ ([N₂₂₂₂][MES]) to 179.77 mg·dm⁻³ ([N₄₄₄₄][CHES]) and taking into account the limits and classifications imposed by the European Legislation (EC₅₀ > 100 mg·dm⁻³).⁵⁷ It should be further stressed that in the case of the GB-ILs [N₁₁₁₁][MES] and [N₁₁₁₁][TES], the bacteria, even when exposed to the maximum concentration tested (≈ 50 g·dm⁻³), has not suffered 50% of inhibition of its luminescence.

Herein, the biocompatible character of the GB-ILs prepared is discussed in three complementary directions: the study of the impact of each structural component of the ILs, namely the cation ([Emim]⁺ vs. [N₂₂₂₂]⁺), the alkyl side chain length ([N₁₁₁₁]⁺ vs. [N₂₂₂₂]⁺ vs. [N₄₄₄₄]⁺) and the anion ([HEPES]⁻ vs. [TES]⁻ vs. [MES]⁻ vs. [CHES]⁻ vs. [Tricine]⁻), on the toxicity. Moreover, a comparison of the bacterial toxicity levels of GBs vs. GB-ILs is also presented.

Having into account the cation core, the results show that the ammonium-based compounds are less toxic than the

imidazolium-based counterparts. Ammonium-based ILs have been previously reported as being less toxic than imidazolium,⁵⁸⁻⁶¹ being the toxic effects of the imidazolium cation mainly attributed to its aromaticity.^{59, 60, 62} The influence of the alkyl side chain length on the toxicity of ammonium-based GB-ILs follows the “side chain effect” thumb rule of toxicity,^{62, 63} i.e. the longer the alkyl chain the more toxic is the compound. Even though the difference between the EC₅₀ results for [N₁₁₁₁]⁺ and [N₂₂₂₂]⁺ for most GB-ILs is not significant, likely due to a superposition of the anion effect in particular for the [CHES]⁻ and [Tricine]⁻ (the most toxic anions) when the length of the alkyl side chains increases to four carbons ([N₄₄₄₄]⁺) the EC₅₀ values decrease considerably. The well-known “side chain effect”^{62, 63} results from the higher hydrophobicity/lipophilicity of the [N₄₄₄₄]⁺ cation, which drives higher interactions with the phospholipid bilayer of the organisms membranes. Unlike most studies that report the anion as a minor feature on the toxicity of ILs,^{56, 64-66} due to the more pronounced effects of the cation on the toxicity towards *Vibrio fischeri*, it is possible to identify here a well-defined trend of the anion influence: [MES]⁻ < [TES]⁻ < [HEPES]⁻ < [Tricine]⁻ < [CHES]⁻.

A comparative study between the GBs and the GB-ILs, shows the Good's buffers to be, in general, even less toxic than their GB-ILs counterparts, as indicated by the EC₅₀ values

shown in Table 4. The addition of a cation core to the GB structure to increase their solubility in organic solvents enhances also their hydrophobicity and, with it, their toxicity. However, some exceptions to this behaviour are identified, that include all the GB-ILs with the anion [MES]⁻ and the GB-ILs [N₁₁₁₁][TES], [N₂₂₂₂][TES] and [Emim][TES]. In those cases, it was possible to increase the EC₅₀ values by up to 2 orders of magnitude (for instance MES, the most toxic GB, presents an EC₅₀ = 214.74 mg·dm⁻³, while the EC₅₀ of [N₂₂₂₂][MES] is 44302.87 mg·dm⁻³).

Conclusions

Herein we have synthesized a new series of ionic liquids based on Good's buffers (Tricine, TES, HEPES, MES, and CHES), here named Good's buffer ionic liquids (GB-ILs) *via* a simple and green neutralization method in aqueous media. The Good's buffers were chosen to act as anions combined with 1-ethyl-3-methylimidazolium, tetramethylammonium, tetraethylammonium and tetrabutylammonium cations. These new ILs offer a high self-buffering capacity in the physiological pH range and a greater protein stability as compared to the corresponding and more conventional ILs, such as [N₁₁₁₁]⁺Br⁻, [N₂₂₂₂]⁺Br⁻, [N₄₄₄₄]⁺Br⁻, and [Emim]⁺Br⁻. Furthermore, their working pH range can be adjusted by the adequate choice of the anion (GB). The polarity and hydrophobicity of GB-ILs can be tuned by the choice of the organic cation. Two universal GB/GB-IL buffers have been formulated to cover a wide pH range for use in enzyme activity assays. Besides all the above benefits of GB-ILs, including their non-toxicities, it was found that these ILs can be further used to prepare aqueous biphasic systems for separation and extraction routes. We have determined the experimental phase diagrams of several aqueous biphasic systems, and their extraction performance for BSA was evaluated. The obtained results confirm that the use of GB-ILs-based ABS for the separation and extraction of biomolecules is a highly promising technique and worthy of further investigation. Studies on further applications of the synthesized IL-GBs are ongoing. Their advantageous characteristics here reported coupled to their simple preparation encourages their future use in industrial applications.

Acknowledgements

Authors are thankful to FCT - *Fundação para a Ciência e a Tecnologia* for financial support through the post-doctoral grants of M. Taha and S.P.M. Ventura, SFRH/BPD/78441/2011 and SFRH/BPD/79263/2011, respectively. CICECO is being funded by FCT through the Pest-C/CTM/LA0011/2013 project. The authors are also grateful to FCT under the scope of the project PTDC/AAC-AMB/119172/2010. M.G. Freire acknowledges the European Research Council (ERC) for the Grant ERC-2013-StG-337753.

* E-mail address: jcoutinho@ua.pt (J.A.P. Coutinho)

Tel.: +351 234 401 507; fax: +351 234 370 084.

Departamento de Química, CICECO, Universidade de Aveiro, 3810-193, Aveiro, Portugal.

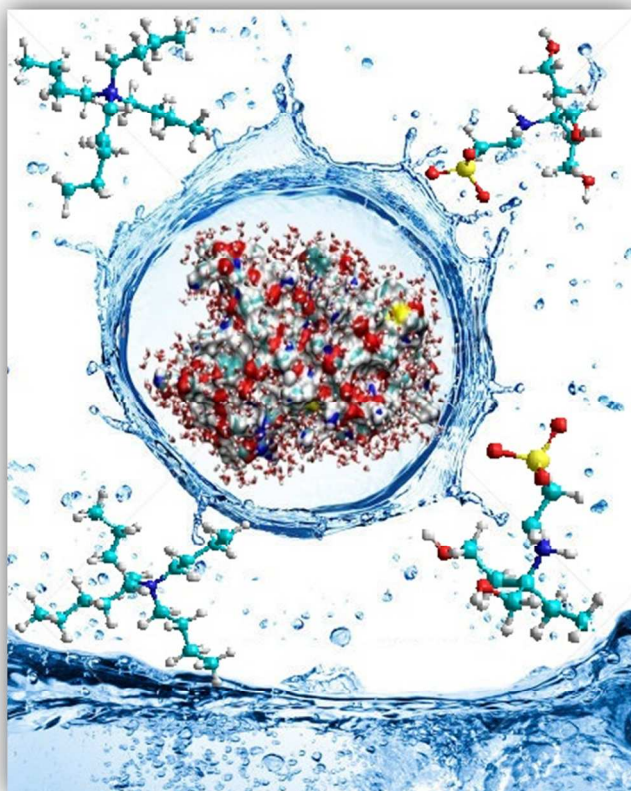
†Electronic Supplementary Information (ESI) available: Tables of characterization of GB-ILs, mid-point pH, buffering pH range, and buffer capacity; figures showing the synthesis pathway, pH profiles, BSA denaturation profiles, and phase diagrams; tables with the binodal data. See DOI: 10.1039/b000000x/

Notes and references

1. T. Welton, *Chem. Rev.*, 1999, **99**, 2071-2084.
2. C. Wang, Y. Guo, X. Zhu, G. Cui, H. Li and S. Dai, *Chem. Commun.*, 2012, **48**, 6526-6528.
3. M. G. Freire, A. F. M. Claudio, J. M. M. Araujo, J. A. P. Coutinho, I. M. Marrucho, J. N. C. Lopes and L. P. N. Rebelo, *Chem. Soc. Rev.*, 2012, **41**, 4966-4995.
4. Q. Miao, S. Zhang, H. Xu, P. Zhang and H. Li, *Chem. Commun.*, 2013, **49**, 6980-6982.
5. I. Khimji, K. Doan, K. Bruggeman, P.-J. J. Huang, P. Vajha and J. Liu, *Chem. Commun.*, 2013, **49**, 4537-4539.
6. S. Cantone, U. Hanefeld and A. Basso, *Green Chem.*, 2007, **9**, 954-971.
7. N. Debeljuh, C. J. Barrow, L. Henderson and N. Byrne, *Chem. Commun.*, 2011, **47**, 6371-6373.
8. A. Kumar and P. Venkatesu, *Chem. Rev.*, 2012, **112**, 4283-4307.
9. J. Lin Huang, M. E. Noss, K. M. Schmidt, L. Murray and M. R. Bunagan, *Chem. Commun.*, 2011, **47**, 8007-8009.
10. M. C. Gurau, S.-M. Lim, E. T. Castellana, F. Albertorio, S. Kataoka and P. S. Cremer, *J. Am. Chem. Soc.*, 2004, **126**, 10522-10523.
11. H. I. Okur, J. Kherb and P. S. Cremer, *J. Am. Chem. Soc.*, 2013, **135**, 5062-5067.
12. H. Zhao, *J. Chem. Technol. Biotechnol.*, 2010, **85**, 891-907.
13. D. R. MacFarlane, R. Vijayaraghavan, H. N. Ha, A. Izgorodin, K. D. Weaver and G. D. Elliott, *Chem. Commun.*, 2010, **46**, 7703-7705.
14. G. Ou, J. Yang, B. He and Y. Yuan, *J. Mol. Catal. B: Enzym.*, 2011, **68**, 66-70.
15. G.-n. Ou, M.-x. Zhu, J.-r. She and Y.-z. Yuan, *Chem. Commun.*, 2006, **0**, 4626-4628.
16. L. Xu, G. Ou and Y. Yuan, *J. Organomet. Chem.*, 2008, **693**, 3000-3006.
17. N. E. Good, G. D. Winget, W. Winter, T. N. Connolly, S. Izawa and R. M. M. Singh, *Biochemistry-US*, 1966, **5**, 467-477.
18. B. S. Gupta, M. Taha and M.-J. Lee, *Process Biochem.*, 2013, **48**, 1686-1696.
19. M. Taha, B. S. Gupta, I. Khoiroh and M.-J. Lee, *Macromolecules*, 2011, **44**, 8575-8589.
20. M. Taha and M.-J. Lee, *Phys. Chem. Chem. Phys.*, 2010, **12**, 12840-12850.
21. M. Taha, I. Khoiroh and M.-J. Lee, *J. Phys. Chem. B*, 2012, **117**, 563-582.
22. M. Taha and M.-J. Lee, *J. Chem. Phys.*, 2013, **138**, 244501-244513.
23. M. Nakano, H. Tateishi-Karimata, S. Tanaka and N. Sugimoto, *J. Phys. Chem. B*, 2013.
24. S. M. Steinberg, E. J. Poziomek, W. H. Engelmann and K. R. Rogers, *Chemosphere*, 1995, **30**, 2155-2197.

25. M. Corporation, *Microtox® manual—a toxicity testing handbook*. Microbics Corporation, 1992, **Carlsbad**, 1–5.
26. M. G. Freire, C. M. S. S. Neves, J. N. Canongia Lopes, I. M. Marrucho, J. A. P. Coutinho and L. P. N. Rebelo, *J. Phys. Chem. B* 2012, **116**, 7660-7668.
27. T. Mourão, A. F. M. Cláudio, I. Boal-Palheiros, M. G. Freire and J. A. P. Coutinho, *J. Chem. Thermodyn.*, 2012, **54**, 398-405.
28. J. C. Merchuk, B. A. Andrews and J. A. Asenjo, *J. Chromatogr. B*, 1998, **711**, 285-293.
29. A. Environmental, *Carlsbad CA, USA*, 1998.
30. O. Trott and A. J. Olson, *J. Comp. Chem.*, 2010, **31**, 455-461.
31. K. A. Majorek, P. J. Porebski, A. Dayal, M. D. Zimmerman, K. Jablonska, A. J. Stewart, M. Chruszcz and W. Minor, *Mol. Immunol.*, 2012, **52**, 174-182.
32. M. J. T. Frisch, G. W.; Schlegel, H. B.; Scuseria, G. E.; Robb, M. A.; Cheeseman, J. R.; Scalmani, G.; Barone, V.; Mennucci, B.; Petersson, G. A.; Nakatsuji, H.; Caricato, M.; Li, X.; Hratchian, H. P.; Izmaylov, A. F.; Bloino, J.; Zheng, G.; Sonnenberg, J. L.; Hada, M.; Ehara, M.; Toyota, K.; Fukuda, R.; Hasegawa, J.; Ishida, M.; Nakajima, T.; Honda, Y.; Kitao, O.; Nakai, H.; Vreven, T.; Montgomery, J. A., Jr.; Peralta, J. E.; Ogliaro, F.; Bearpark, M.; Heyd, J. J.; Brothers, E.; Kudin, K. N.; Staroverov, V. N.; Kobayashi, R.; Normand, J.; Raghavachari, K.; Rendell, A.; Burant, J. C.; Iyengar, S. S.; Tomasi, J.; Cossi, M.; Rega, N.; Millam, N. J.; Klene, M.; Knox, J. E.; Cross, J. B.; Bakken, V.; Adamo, C.; Jaramillo, J.; Gomperts, R.; Stratmann, R. E.; Yazyev, O.; Austin, A. J.; Cammi, R.; Pomelli, C.; Ochterski, J. W.; Martin, R. L.; Morokuma, K.; Zakrzewski, V. G.; Voth, G. A.; Salvador, P.; Dannenberg, J. J.; Dapprich, S.; Daniels, A. D.; Farkas, Ö.; Foresman, J. B.; Ortiz, J. V.; Cioslowski, J.; Fox, D. J., Gaussian 09, Gaussian, Inc., Wallingford CT, 2009.
33. T. V. a.d.o.U.o.K.a.F.K.G., 1989–2007, 25 GmbH, since 2007; available from <http://www.turbomole.com>.
34. K. Fukumoto, M. Yoshizawa and H. Ohno, *J. Am. Chem. Soc.*, 2005, **127**, 2398-2399.
35. H. Ohno and K. Fukumoto, *Acc. Chem. Res.*, 2007, **40**, 1122-1129.
36. D. A. Ellis, *Nature*, 1961, **191**, 1099-1100.
37. T. Peters Jr, *All about albumin: biochemistry, genetics, and medical applications*, Academic press, 1995.
38. J. Ye, F. Fan, X. Xu and Y. Liang, *Food Res. Int.*, 2013, **53**, 449-455.
39. D. M. Charbonneau and H.-A. Tajmir-Riahi, *J. Phys. Chem. B* 2009, **114**, 1148-1155.
40. K. Murayama and M. Tomida, *Biochem. Eng. J.*, 2004, **43**, 11526-11532.
41. S. Ghosh, S. Jana and N. Guchhait, *J. Phys. Chem. B*, 2011, **116**, 1155-1163.
42. O. Gursky and S. Aleshkov, *Biochimica et Biophysica Acta (BBA) - Protein Structure and Molecular Enzymology*, 2000, **1476**, 93-102.
43. M. J. Holden, M. P. Mayhew, D. T. Gallagher and V. L. Vilker, *Biochimica et Biophysica Acta (BBA) - Protein Structure and Molecular Enzymology*, 2002, **1594**, 160-167.
44. A. M. Tsai, J. H. van Zanten and M. J. Betenbaugh, *Biotechnology and Bioengineering*, 1998, **59**, 273-280.
45. A. M. Tsai, J. H. van Zanten and M. J. Betenbaugh, *Biotechnology and Bioengineering*, 1998, **59**, 281-285.
46. S. Ghosh and N. Guchhait, *Photochem. Photobiol.*, 2010, **86**, 290-296.
47. H. Benyamini, A. Shulman-Peleg, H. J. Wolfson, B. Belgorodsky, L. Fadeev and M. Gozin, *Bioconjugate Chem.*, 2006, **17**, 378-386.
48. A. Michnik, K. Michalik and Z. Drzazga, *J. Therm. Anal. Calorim.*, 2005, **80**, 399-406.
49. K. E. Gutowski, G. A. Broker, H. D. Willauer, J. G. Huddleston, R. P. Swatloski, J. D. Holbrey and R. D. Rogers, *J. Am. Chem. Soc.*, 2003, **125**, 6632-6633.
50. J. F. B. Pereira, F. Vicente, V. C. Santos-Ebinuma, J. M. Araújo, A. Pessoa, M. G. Freire and J. A. P. Coutinho, *Process Biochem.*, 2013, **48**, 716-722.
51. A. F. M. Cláudio, A. M. Ferreira, C. S. R. Freire, A. J. D. Silvestre, M. G. Freire and J. A. P. Coutinho, *Sep. Purif. Technol.*, 2012, **97**, 142-149.
52. C. M. S. S. Neves, J. F. O. Granjo, M. G. Freire, A. Robertson, N. M. C. Oliveira and J. A. P. Coutinho, *Green Chem.*, 2011, **13**, 1517-1526.
53. H. Passos, A. C. A. Sousa, M. R. Pastorinho, A. J. A. Nogueira, L. P. N. Rebelo, J. A. P. Coutinho and M. G. Freire, *Anal. Methods*, 2012, **4**, 2664-2667.
54. S. P. M. Ventura, R. L. F. de Barros, J. M. de Pinho Barbosa, C. M. F. Soares, A. S. Lima and J. A. P. Coutinho, *Green Chem.*, 2012, **14**, 734-740.
55. H. Passos, A. R. Ferreira, A. F. M. Cláudio, J. A. P. Coutinho and M. G. Freire, *Biochem. Eng. J.*, 2012, **67**, 68-76.
56. S. P. M. Ventura, C. S. Marques, A. A. Rosatella, C. A. M. Afonso, F. Gonçalves and J. A. P. Coutinho, *Ecotoxicol. Environ. Saf.*, 2012, **76**, 162-168.
57. L. Li, J. Xie, S. Yu, Z. Su, S. Liu, F. Liu, C. Xie and B. Zhang, *RSC Adv.*, 2012, **2**, 11712-11718.
58. R. J. Bernot, E. E. Kennedy and G. A. Lamberti, *Environ. Toxicol. Chem.*, 2005, **24**, 1759-1765.
59. D. J. Couling, R. J. Bernot, K. M. Docherty, J. K. Dixon and E. J. Maginn, *Green Chem.*, 2006, **8**, 82-90.
60. C. Pretti, C. Chiappe, I. Baldetti, S. Brunini, G. Monni and L. Intorre, *Ecotox. Environ. Safe.*, 2009, **72**, 1170-1176.
61. X. Wang, C. A. Ohlin, Q. Lu, Z. Fei, J. Hu and P. J. Dyson, *Green Chem.*, 2007, **9**, 1191-1197.
62. S. M. Ventura, A. M. Gonçalves, T. Sintra, J. Pereira, F. Gonçalves and J. P. Coutinho, *Ecotoxicology*, 2013, **22**, 1-12.
63. S. Stolte, M. Matzke, J. Arming, A. Boschen, W.-R. Pitner, U. Welz-Biermann, B. Jastorff and J. Ranke, *Green Chem.*, 2007, **9**, 1170-1179.
64. R. J. Bernot, M. A. Brueseke, M. A. Evans-White and G. A. Lamberti, *Environ. Toxicol. Chem.*, 2005, **24**, 87-92.
65. M. T. Garcia, N. Gathergood and P. J. Scammells, *Green Chem.*, 2005, **7**, 9-14.
66. S. Stolte, J. Arming, U. Bottin-Weber, M. Matzke, F. Stock, K. Thiele, M. Uerdingen, U. Welz-Biermann, B. Jastorff and J. Ranke, *Green Chem.*, 2006, **8**, 621-629.

Table of Contents



Green Chemistry Accepted Manuscript